UNSUPERVISED SEGMENTATION APPLIED ON SONAR IMAGES

M. Mignotte[‡] *C.Collet* [‡] *P.Pérez* [•] *P.Bouthemy* [•]

[‡] Groupe de Traitement du Signal, Ecole Navale, Lanvéoc-Poulmic,
29240 Brest-Naval, France.
email : name@ecole-navale.fr

[•] IRISA/INRIA, Campus Universitaire de Beaulieu, 35042 Rennes cedex, France.
email : name@irisa.fr

Abstract. This work deals with unsupervised sonar image segmentation. We present a new estimation segmentation procedure using the recent iterative method of estimation called Iterative Conditional Estimation (**ICE**) [1]. This method takes into account the variety of the laws in the distribution mixture of a sonar image and the estimation of the parameters of the label field (modeled by a Markov Random Field (**MRF**)). For the estimation step, we use a maximum likelihood technique to estimate the noise model parameters, and the least squares method proposed by Derin *et al.* [2] to estimate the **MRF** prior model. Then, in order to obtain an accurate segmentation map and to speed up the convergence rate, we use a multigrid strategy exploiting the previously estimated parameters. This technique has been successfully applied to real sonar images [1], and is compatible with an automatic processing of massive amounts of data.

1 Introduction

Due to its high-resolution performance a high frequency sonar allows to visualize all kinds of objects located on the sea-bottom. The detection of these objects and their classification (as wrecks, rocks, man-made objects, and so on...) are based on the extraction and the identification of their associated cast shadows in sonar pictures [3]. Before any classification step, one must segment the sonar image between *shadow* areas and *sea-bottom reverberation* areas. Nevertheless, segmenting an image into different classes without *a priori* information is not an easy task in computer vision: the main difficulty is that the estimation of the model parameters introduced is required for the segmentation, while the

[1] Acknowledgements : The authors thank the **GESMA** (Groupe d'Etude Sous-Marine de l'Atlantique) for having provided us with numerous real SONAR pictures and the **DRET** (Direction des Recherches Etudes et Techniques de la DGA) for partial financial support of this work.

segmentation is needed for the parameter estimation. For example a supervised Markovian segmentation [4] [5] gives good results; nevertheless, a substantial number of estimated parameters is usually required in order to solve the difficult problem of unsupervised sonar images segmentation.

To circumvent this difficulty, a scheme was proposed in [6] in which the estimation and the segmentation are implemented recursively. Although the method proved to converge in the case of independent Gaussian model, it is not clear that it can be extended to **MRF** model. Also, the method requires very complicated computations. An alternate approach to solve the unsupervised **MRF** segmentation problem consists in having a two steps process. First, a parameter *estimation step* in which we have to estimate the noise model parameters and the **MRF** model parameters. Then, a second step in which we apply the segmentation algorithm with the estimated parameters.

First, let us consider the estimation of the noise model parameters. There are a number of methods that use the image histogram. Most of them (Fourier, polynomials and cumulate histogram methods) are inefficient in the case of an important distribution mixture and without mathematical justification to estimate a mixture of different laws [7]. Several techniques have been proposed to determine a Maximum Likelihood estimate of the noise model parameters from a given image. **EM** (*Expectation Maximization*) or **SEM** algorithms (*Stochastic Expectation Maximization*) can be used in the case of Gaussian distribution mixtures [8] [9]. In a specific application to sonar imagery, we have taken into account the variety of laws in the distribution mixture [3]. Nevertheless, these algorithms do not account for the properties of the label field defined in a **MRF** segmentation as a Gibbs distribution. As we will show in this paper, another way to estimate these parameters consists in using the **ICE** procedure [1].

Let us consider now the estimation of the **MRF** model parameters. The **MRF** model provides a powerful tool for incorporating the knowledge about the spatial dependence of the labels of the segmented image. The knowledge about the scene is incorporated into an energy function that consists of appropriate clique functions. In most of the previous work using **MRF** models, the parameters of the prior model are assumed to be known and determined in an *ad hoc* fashion. However, the values of these parameters determine the distribution over the configuration space to which the system converges. Besides, in our application, it is difficult to find appropriate values for the clique parameters since the real scenes are different for each picture (sea floor with pebbles, dunes, ridges, sand, ...). Thus, estimating these parameters is very crucial in practice for successful labelling. One way to estimate them from a given image is to use a gradient descent algorithm [10] but this method is slow and very sensitive to the initial value given to initialize the procedure. In [11], the **EM** algorithm is used but this iterative scheme also requires a lot of computing time [12]. Besides these two iterative methods may run into a local maximum without reaching the proper solution. In [13], the authors propose to implement the estimation of the parameters associated with clique functions as a neural network whose weights are learned from examples by the error backpropagation algorithm. This method is interesting but requires a learning step from a sample training data. Let us mention also the use of Metropolis algorithm in [14].

In this paper, we adopt for the *Estimation Step* the **ICE** procedure [1] to estimate simultaneously the **MRF** prior model parameters (with the Least Square estimator **LSQR** described by Derin *et al* [2]) and the noise model parameters (with a Maximum Likelihood estimator). For the *Segmentation Step*, we use a multigrid segmentation with the previously estimated parameters. This paper is organized as follows : In sections 2 and 3, we define the notation and we give a brief description of the **ICE** procedure and the used estimators. Sections 4 and 5 detail the *Estimation Step* and the initialization of the procedure. The experimental results on real scenes are presented in section 6.

2 Iterative Conditional Estimation

We consider a couple of random fields $Z = (X, Y)$, with $Y = \{Y_s, s \in S\}$ the field of observations located on a lattice S of N sites s, and $X = \{X_s, s \in S\}$ the associated label field. Each of the Y_s takes its value in $\Lambda_{obs} = \{0, \ldots, 255\}$ and each X_s in $\{e_0 = shadow,\ e_1 = sea\ bottom\ reverberation\}$. The distribution of (X, Y) is defined by, firstly, $P_X(x)$, the distribution of X which is supposed stationary and Markovian and, secondly, the site-wise likelihoods $P_{Y_s/X_s}(y_s/x_s)$. In this work, these likelihoods depend on the class label x_s. The observable Y is called the *incomplete data* and Z the *complete data*.

In the unsupervised segmentation case, we have to estimate in a first step (*Estimation Step*), parameter vectors Φ_x and Φ_y which define $P_X(x)$ and $P_{Y/X}(y/x)$ respectively. We estimate them using the iterative method of estimation called Iterated Conditional Estimation (**ICE**) [1]. This method requires to find two estimators, namely $\hat{\Phi}_x = \Phi_x(X)$ and $\hat{\Phi}_y = \Phi_y(X, Y)$ for completely observed data. When X is unobservable, the iterative **ICE** procedure defines $\Phi_x^{[k+1]}$ and $\Phi_y^{[k+1]}$ as conditional expectations of $\hat{\Phi}_x$ and $\hat{\Phi}_y$ given $Y = y$, computed according to the current values $\Phi_x^{[k]}$ and $\Phi_y^{[k]}$. These are the best approximations of Φ_x and Φ_y in terms of the mean squares error. By denoting E_k, the conditional expectation using $\Phi^{[k]} = [\Phi_x^{[k]}, \Phi_y^{[k]}]$, this iterative procedure is defined as follows:

- One takes an initial value $\Phi^{[0]} = [\Phi_x^{[0]}, \Phi_y^{[0]}]$.
- $\Phi^{[k+1]}$ is computed from $\Phi^{[k]}$ and $Y = y$ by :

$$\Phi_x^{[k+1]} = E_k[\hat{\Phi}_x | Y = y] \tag{1}$$
$$\Phi_y^{[k+1]} = E_k[\hat{\Phi}_y | Y = y] \tag{2}$$

The computation of these expectations is impossible in practice, but we can approach (1) and (2), thanks to the law of large numbers by:

$$\Phi_x^{[k+1]} = \frac{1}{n} \cdot [\Phi_x(x_{(1)}) + \cdots + \Phi_x(x_{(n)})] \tag{3}$$

$$\Phi_y^{[k+1]} = \frac{1}{n} \cdot [\Phi_y(x_{(1)}, y) + \cdots + \Phi_y(x_{(n)}, y)] \tag{4}$$

where $x_{(i)}$, $i = 1, \ldots, n$ are realizations of X according to the posterior distribution $P_{X/Y, \Phi^{[k]}}(x/y, \Phi^{[k]})$. Finally, we can use the **ICE** procedure for our application because we get:

- An estimator $\Phi_y(X, Y)$ of the *complete data* : we use a Maximum Likelihood (**ML**) estimator for the noise model parameter estimation. In order to estimate $\hat{\Phi}_x = \Phi_x(X)$, given a realization x of X, we use the **LSQR** estimator [2] described by Derin *et al.* which will be summarized in subsection 3.2.
- An initial value $\Phi^{[0]}$ not *too far* from the optimal parameters (see section 4).
- A way of simulating realizations of X according to the posterior distribution $P_{X/Y}(x/y)$ by using the Gibbs sampler [15].

The **ICE** procedure is not limited by the form of the conditional distribution of the noise. This algorithm is well adapted for our application where the speckle distribution in the sonar images is not exactly known and varies according to experimental conditions. Besides, let us recall that this method does not assume the independence of the random variables X_i such as the **SEM** or the **EM** algorithm [8][9] and takes into account the Markovian characteristics of the *a priori* label field.

3 Estimation of the Model Parameters for the complete data

3.1 Noise Model Parameters

The Gaussian law, $\mathcal{N}(\mu, \sigma^2)$, is an appropriate degradation model to describe the luminance y within *shadow* regions (essentially due to the electronical noise). The most natural choice of the estimator $\hat{\Phi}_y = \Phi_y(x = e_0, y)$ is the empirical mean and the empirical variance. If N_0 pixels are located in the shadow areas, we have:

$$\hat{\mu}_{ML} = \frac{1}{N_0} \cdot \sum_{s:x_s=e_0} y_s \tag{5}$$

$$\hat{\sigma}^2_{ML} = \frac{1}{N_0 - 1} \cdot \sum_{s:x_s=e_0} (y_s - \hat{\mu}_{ML})^2 \tag{6}$$

In order to take into account the speckle noise phenomenon [16], we model the conditional density function of the *sea bottom* class by a shifted Rayleigh law $\mathcal{R}(min, \alpha^2)$ [3] :

$$P(y_s/x_s = e_1) = \frac{y_s - min}{\alpha^2} \cdot \exp\left[-\frac{(y_s - min)^2}{2\alpha^2}\right]$$

The maximum value of the log-likelihood function is used to determine a Maximum Likelihood estimator of the *complete data*. If $\hat{y}_{min}$ is the minimum grey level in the *sea bottom* areas and N_1 the number of pixels located within the *sea bottom* regions, we obtain the following results:

$$\hat{\alpha}^2_{ML} = \frac{1}{2N_1} \cdot \sum_{s:x_s=e_1} (y_s - \widehat{min}_{ML})^2 \qquad (7)$$

$$\widehat{min}_{ML} \approx \hat{y}_{min} - 1 \qquad (8)$$

In the two cases, π_k (the proportion of the kth class) is given by the empirical frequency:

$$\hat{\pi}_k = \frac{N_k}{N_o + N_1} \qquad k \in \{0, 1\}$$

3.2 A Priori Model Parameters

A **MRF** prior model is specified in terms of parameters, called the clique parameters. These parameters correspond to the clique potential values of an equivalent Gibbs Random Field representation. Several schemes have been proposed in the computer vision literature for the estimation of the **MRF** parameters. We can cite the coding and the maximum pseudo likelihood method proposed by Besag in [4]. Let us also mention the stochastic gradient method converging to the maximum of the likelihood developped in [17]. These methods offer a rigorous mathematical justification, but they are iterative and have to solve a set of non-linear equations. This means that they require an initial guess for the solution and may run into a local maximum without reaching the proper solution.

The **MRF** parameter estimation method described in this section has been proposed by Derin *et al.* This scheme is not iterative and parameters estimated are close to the optimal parameters [2]. We briefly describe this estimator in terms of our model, *i.e.*, with respect to the 2^{nd} order neighborhood system. Let X_{ν_s} represent the set of labels assigned to the neighbors of site s and $\Phi_x = [\beta_1, \beta_2, \beta_3, \beta_4]$ be the *a priori* parameter vector corresponding to two-site clique potentials (see **Fig. 1**).

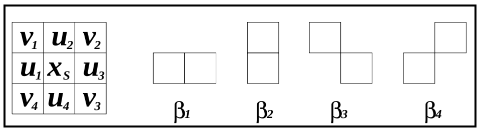

Fig. 1. 2^{nd} *order neighborhood and two-site associated cliques.*

We define:

$$\Theta^{\mathbf{t}}(x_s, \eta_s) = [\mathcal{I}(x_s, u_1) + \mathcal{I}(x_s, u_3), \mathcal{I}(x_s, u_2) + \mathcal{I}(x_s, u_4), \mathcal{I}(x_s, v_1) + \mathcal{I}(x_s, v_3), \mathcal{I}(x_s, v_2) + \mathcal{I}(x_s, v_4)]$$

$$\text{Where} \qquad \mathcal{I}(z_1, z_2) = \begin{cases} 0 \text{ if } z_1 = z_2, \\ 1 \text{ otherwise.} \end{cases}$$

The local energy function U_s can be expressed as:

$$U_s(x_s, \eta_s, \Phi_x) = \Theta^t(x_s, \eta_s)\Phi_x \tag{9}$$

The prior local conditional probability at site s can be written as:

$$P_{X_s/X_{\nu_s}}(x_s/\eta_s) = \frac{P_{X_s, X_{\nu_s}}(x_s, \eta_s)}{P_{X_{\nu_s}}(\eta_s)} = Z_s^{-1} \cdot \exp^{-U_s(x_s, \eta_s, \Phi_x)}$$

Where Z_s is the local partition function and $P(e_1, \eta_s)$ is the joint distribution of the label e_1 with the neighborhood η_s. We obtain the following expression for the two different values of x_s ($x_s = e_0$ and $x_s = e_1$) with identical neighborhood η_i:

$$\exp[-U(e_1, \eta_i, \Phi_x) + U(e_0, \eta_i, \Phi_x)] = \frac{P_{X_s, X_{\nu_s}}(e_1, \eta_i)}{P_{X_s, X_{\nu_s}}(e_0, \eta_i)}$$

Taking logarithms on both sides and substituting for U from (9), we have:

$$[\Theta(e_0, \eta_i) - \Theta(e_1, \eta_i)]^t \Phi_x = \ln\left[\frac{P_{X_s, X_{\nu_s}}(e_1, \eta_i)}{P_{X_s, X_{\nu_s}}(e_0, \eta_i)}\right] \tag{10}$$

Φ_x is the unknown parameter vector to be estimated and the ratio of the right hand side of (10) may be estimated using simple histogramming (by counting the number of 3×3 blocks of type (e_1, η_i) and dividing by the number of blocks of type (e_0, η_i) over the image). By substituting for each value of η_i in (10), we obtain 256 equations (2^8 possible neighborhood configurations) in four unknowns. A specific combination (e_j, η_i) may not exist. In this case we cannot obtain a linear equation because of the logarithm in (10). Moreover $\Theta(e_0, \eta_i)$ $= \Theta(e_1, \eta_i)$ implies equations of type $0 = C^{st}$, therefore we ignore those types of equations too. This overdetermined linear system of equations is solved with the least squares method.

We present some examples of the parameters estimation of a Gibbs Distribution (**GD**) using realizations that are generated with specified values. The estimates are compared to the specified values of the parameters in Table 1. Realizations of **GD** are presented in Figure 2.

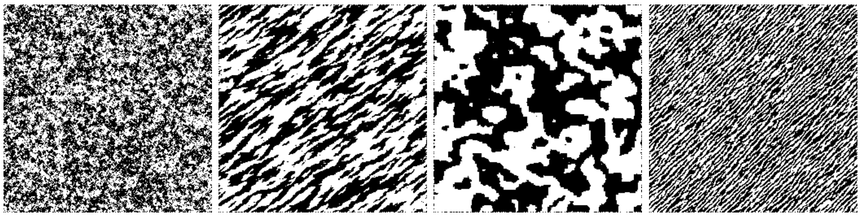

(a) (b) (c) (d)

Fig. 2. *Realizations of* **GD** *with specified parameters (see* **Table 1** *for parameters values).*

Fig	Φ_x	β_1	β_2	β_3	β_4
(**a**)	Φ_x	0.3	0.3	0.3	0.3
	$\hat{\Phi}_x$	0.3	0.29	0.31	0.31
(**b**)	Φ_x	2	1	-1	1
	$\hat{\Phi}_x$	1.77	0.94	-0.86	0.98
(**c**)	Φ_x	2	2	0	0
	$\hat{\Phi}$	1.93	1.94	-0.05	0.01
(**d**)	Φ_x	1	1	-1	1
	$\hat{\Phi}$	0.95	0.93	-0.96	1.03

Table 1. *Specified (Φ_x) and estimated parameters ($\hat{\Phi}_x$). $\beta_1, \beta_2, \beta_3, \beta_4$ designate the potentials associated with the horizontal, vertical, right diagonal, left diagonal cliques.*

Synthetic textures created in Figure 2 show that the Gibbs Random Field representation is an appropriate spatial distribution to model the *a priori* label field distribution. Figure 2.*a* shows inhomogeneous shapes such as segmented pebbly sea bottom. Figure 2.*b* and 2.*c* depict homogeneous shapes respectively with a dominant orientation representative of segmented dunes (2.*b*) or with geometric shapes as for the shadows of manufactured objects (2.*c*). Figure 2.*d* looks like segmented real scenes containing ridges of sand.

Parameter variation for a **GD** class gives a wide range of texture realizations. Those presented are only a few samples. These experiments demonstrate that estimated parameters are close to the true parameters.

4 Initialization

The initial parameter values have a significant impact on the rapidity of the convergence of the **ICE** procedure and on the quality of the final estimates. In our application, we use the following method: The initial parameter of the noise model $\Phi_y^{[0]}$ are determined by applying a small non overlapping sliding window over the image and calculating the sample mean, variance and minimum grey level estimates. Each estimation calculated over the sliding window thus gives a sample $\mathbf{x}_i$, (*i.e* a three component vector). These samples $\{\mathbf{x}_1, \ldots, \mathbf{x}_M\}$ are then clustered into two classes $\{e_0, e_1\}$ using the **K-means** clustering procedure. This algorithm uses a similarity measure that is the Euclidean distance of the samples and a criterion J defined by:

$$J = \sum_{i=1}^{K} \sum_{\mathbf{x}_l \in C_i} \mid \mathbf{x}_l - c_i \mid^2$$

where the second sum is over all samples in the ith cluster and c_i is the *center* of the cluster. It is easily seen that for a given set of samples and class assignements, J is minimized by choosing c_i to be the *sample mean* of the ith cluster. Moreover, when c_i is the sample mean, J is minimized by assigning $\mathbf{x}_j$ to the class of the cluster with the nearest mean. A number of other criteria are given in [18]. The complete algorithm is outlined below:

1. Choose K initial cluster centres $c_1^{[1]}, \ldots, c_K^{[1]}$. These could be arbitrarily, but are usually defined by:

$$c_i^{[1]} = \mathbf{x}_i \qquad 1 \leq i \leq K$$

2. At the k^{th} step, assign the sample $\mathbf{x}_l$, $1 \leq l \leq M$ to cluster i if

$$\| \mathbf{x}_l - c_i^{[k]} \| < \| \mathbf{x}_l - c_j^{[k]} \| \qquad \forall \quad j \neq i$$

In fact, we reassign every sample to the cluster with the nearest mean. In our application, the measure of similarity between two samples is the Euclidean distance. In the case of equality, we assign $\mathbf{x}_l$ arbitrarily to i or j.

3. Let $C_i^{[k]}$ denote the i^{th} cluster after Step 2. Determine new cluster centres by:

$$c_i^{[k+1]} = \frac{1}{N_i} \cdot \sum_{\mathbf{x} \in C_i^{[k]}} \mathbf{x}$$

where N_i = number of samples in $C_i^{[k]}$. Thus, the new cluster centre is the mean of the samples in the old cluster.

4. Repeat until convergence is achieved ($c_i^{[k+1]} = c_i^{[k]}\ \forall i$).

Although it is possible to find pathological cases where convergence never occurs [18], the algorithm does converge in all tested examples. The rapidity of convergence depends on the number K, of cluster centers chosen, the choice of initial cluster centers and the order in which the samples are considered. In our application $K = 2$.

Figure 3.a represents a sonar image and the result of the K-means clustering algorithm is reported in Figure 3.b. Figure 3.c shows the representation of the

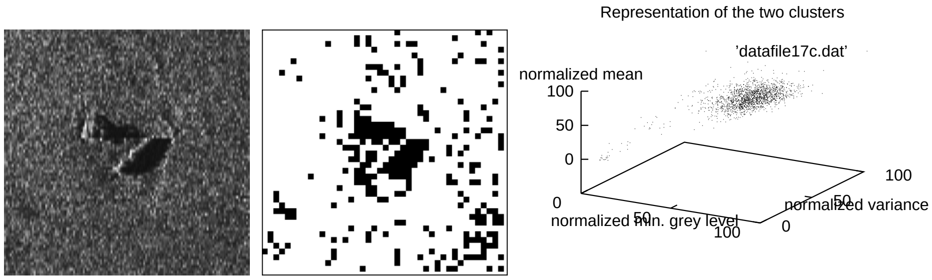

Fig a: *sonar picture (object and rock shadows)* **Fig b**: *K-means clustering procedure* **Fig c**: *representation of the two clusters*

Fig. 3.

two clusters associated to the *shadow* class and *sea bottom reverberation* class. Each sample $\mathbf{x}_l$ is represented by a point.

ML estimation is then used over the K-means segmentation to find $\Phi_y^{[0]}$. On one hand, a small size window can increase the accuracy of the segmentation and then the precision of the distribution mixture estimation. On the other hand, it decreases the number of pixels with which $\mathbf{x}_l$'s are computed and can increase the misclassification error. In our application, good results are obtained with a $6 * 6$ pixels window.

The initial parameters of the Gibbs distribution are obtained by using the **LSQR** method from the **ML** segmentation $\hat{x}^{[0]}$.

$$\Phi_x^{[0]} = \Phi_{\text{LSQR}}(\hat{x}^{[0]}) \quad \text{with} \quad \hat{x}_s^{[0]} = \arg\max_{x_s} P_{Y_s/X_s,\Phi_y^{[0]}}(y_s/x_s, \Phi_y^{[0]}) \quad (\forall s \in S)$$

5 Parameters Estimation Procedure for the incomplete data

We can use the following algorithm to solve the unsupervised sonar image segmentation problem. Let us remind that this method takes into account the diversity of the laws in the distribution mixture estimation as well as the problem of the estimation of the label field parameters.

- **Parameter Initialization**: K-mean algorithm (see section 4). Let us denote $\Phi^{[0]} = [\Phi_x^{[0]}, \Phi_y^{[0]}]$, the obtained result.
- **ICE procedure**:
  $\Phi^{[k+1]}$ is computed from $\Phi^{[k]}$ in the following way:
  $\triangleright$ Using the Gibbs sampler, n realizations $x_{(1)}, \ldots, x_{(n)}$ are simulated according to the posterior distribution with parameter vector $\Phi^{[k]}$, with:

$$P_{Y_s/X_s}(y_s/x_s = e_0) \quad \text{a Gaussian law} \quad \text{(shadow area)}$$
$$P_{Y_s/X_s}(y_s/x_s = e_1) \quad \text{a shifted Rayleigh law} \quad \text{(sea bottom area)}$$

▷ For each $x_{(i)}$ $(i = 1, \ldots, n)$, the parameter vector Φ_x is estimated by the Derin *et al.* algorithm and Φ_y with the **ML** estimator of each class.
▷ $\Phi^{[k+1]}$ is obtained from $(\Phi_x(x_{(i)}), \Phi_y(x_{(i)}, y)) \quad 1 \leq i \leq n$ by (3) and (4).

If the sequence $\Phi^{[k]}$ becomes steady, the **ICE** procedure is ended and one proceeds to the segmentation using the estimated parameters.

In order to estimate the *min* parameter of the *sea bottom reverberation* class during the **ICE** procedure, we can associate a very low probability for the pixels in the sonar image with a grey level equal to *min* [12].

We can regulate the importance of the "*stochastic*" aspect of the **ICE** by choosing n. When n increases, the "*stochastic*" side of the algorithm decreases. The intentional choice of a small value for n ($n = 1$ in our application) can increase its efficiency [19]. In [12], we have shown the superiority of the **ICE** procedure over the **EM** or **SEM** algorithm in case of different distributions mixture estimation or Rayleigh law mixture estimation. We have shown also that the estimation of the noise model parameters Φ_y was better according to the Kolmogorov distance or χ^2 error [12], when Φ_x and Φ_y are jointly estimated.

The Figure 4 represents the mixture of distributions of the sonar image shown in section 4, and the convergence of the estimation of the *a priori* parameters can be seen in Figure 4.b. The obtained results are given in Table 2.

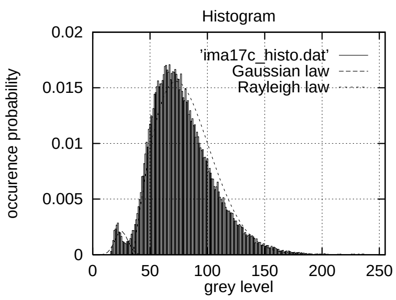

Fig a: *Image histogram of the picture reported in Figure 3.a and estimated mixture*

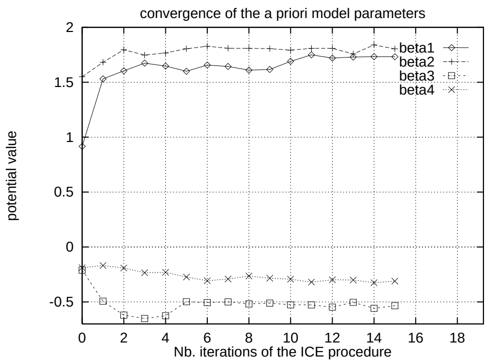

Fig b: *Convergence of the estimation of the a priori parameters*

Fig. 4.

The quality of the estimations is difficult to appreciate in absence of the real values. We can roughly perform such an evaluation by comparing the image histogram with the probability densities mixture corresponding to the estimated parameters. Figure 4.a shows the resulting mixture solution in graphical

	Initialization : **K-means**			
$\hat{\Phi}^{[0]}_{y_{(shadow)}}$	$0.16_{(\pi)}$	$55_{(\mu)}$	$286_{(\sigma^2)}$	
$\hat{\Phi}^{[0]}_{y_{(sea-bottom)}}$	$0.84_{(\pi)}$	$37_{(min)}$	$952_{(\alpha^2)}$	
$\hat{\Phi}^{[0]}_{x}$	$0.9_{(\beta_1)}$	$1.6_{(\beta_2)}$	$-0.2_{(\beta_3)}$	$-0.2_{(\beta_4)}$

	ICE procedure			
$\hat{\Phi}_{y_{(shadow)}}$	$0.03_{(\pi)}$	$25_{(\mu)}$	$32_{(\sigma^2)}$	
$\hat{\Phi}_{y_{(sea-bottom)}}$	$0.97_{(\pi)}$	$35_{(min)}$	$1424_{(\alpha^2)}$	
$\hat{\Phi}_{x}$	$1.7_{(\beta_1)}$	$1.8_{(\beta_2)}$	$-0.6_{(\beta_3)}$	$-0.3_{(\beta_4)}$

Estimated parameters on the picture reported in Figure 3.a. π stands for the proportion of the two classes within the sonar image. μ and σ^2 are the Gaussian parameters (shadow area). min and α are the Rayleigh law parameters (sea floor reverberation). β_i's are the a priori parameters of the Markovian modeling. $\Phi^{[0]}$ represents the initial parameter estimates and the final estimates are denoted $\hat{\Phi}$.

Table 2.

form. The two dashed curves in the figures represent the individual components $P_{Y/X_i}(y/e_m)(0 \leq m < K)$. The histogram is quite close to the mixture densities based on the estimated parameters, and a segmentation with these estimates (see section 6) gives good results.

6 Segmentation on Real Pictures

The segmentation of sonar images in two classes is stated as a statistical labelling problem according to a global Bayesian formulation in which the posterior distribution $P_{X/Y,\Phi}(x/y,\phi) \propto \exp -U(x,y)$ has to be maximized. The corresponding energy function to be minimized is of the form:

$$U(x,y) = \underbrace{\sum_{s \in S} \Psi_s(x_s,y_s)}_{U_1(x,y)} + \underbrace{\sum_{<s,t>} \beta_{s,t}\ \mathcal{I}(x_s,x_t)}_{U_2(x)}$$

where U_1 expresses the adequacy between observations and labels ($\Psi_s(x_s,y_s) = -\ln P(y_s/x_s)$), and U_2 the energy of the *a priori* model ($\beta_{s,t} = \beta_1, \beta_2, \beta_3$, or β_4 according to the type of neighboring pair $< s,t >$). The energy function is complex and the **MAP** (Maximum a Posteriori) solution is difficult to estimate. In order to avoid local minima and to speed up the convergence rate, we use a multigrid strategy [20]. The observation field remains at the finest resolution, only the **MRF** model will be hierarchically defined. The energy function is rewritten at each scale as a coarser **MRF** model.

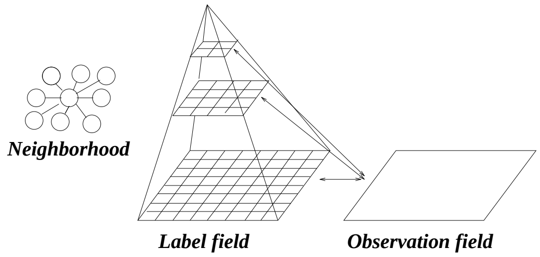

Fig. 5. *Neighborhood system and the multiscale relaxation structure.*

To generate the multigrid **MRF** model, the grid S is hierarchically partitioned into N_i sets b_k^l (with $k \in \{1 \dots N_i\}$) of size $2^l \times 2^l$. We consider that the label x_k^l assigned to a block b_k^l is constant over all the pixels of the block. Given this constraint, an energy $U^l(x^l, y)$ can be easily derived from the original one by rewritting and properly grouping terms of $U(x, y)$ when x is actually block-wise constant relative to the partition ($\forall p \in b_k^l, x_p = x_k^l$) [5][20] :

$$\begin{aligned} & U^l(x^l, y) = U_1^l(x^l, y) + U_2^l(x^l) \\ \text{with} \quad & U_1^l(x^l, y) \triangleq \sum_{s \in S^l} \Psi_s^l(x_s^l, y_{b_s^l}) = \sum_{k=1}^{N^l} \sum_{p \in b_k^l} \Psi_s^l(x_k^l, y_p) \\ \text{and} \quad & U_2^l(x^l) = \sum_{<k,m>} \beta_{k,m}^l \, \mathcal{I}(x_k^l, x_m^l) \end{aligned}$$

where $y_{b_k^l}$ stands for the set of all the observations of the cell b_k^l and $\beta_{k,m}^l$ are deduced from the β_i's [20]. For propagating information through scale, we use a *coarse to fine* minimization strategy: in order to minimize the energy function associated with the **MRF** model at each scale, we use the **ICM** algorithm [4]; The final estimate obtained at a given level is interpolated to be used as an initialization for the relaxation process at the next finer level.

The segmentation result obtained for the image shown in Figure 6.a is reported in Figure 6.b.

We have presented in Figure 7 and 8 the different steps of two other unsupervised segmentation on real sonar images. Figures 7.a and 8.a represent two original observations. Figures 7.b and 8.b show the result of the K-means clustering algorithm and Figures 7.c and 8.c, the representation of the two clusters associated to the *shadow* class and *sea-bottom* class. The mixture of distributions is represented by Figures 7.d and 8.d and the final result of the segmented image is reported in Figures 7.e and 8.e. The obtained results are given in Table 3 and Table 4.

One can see that this approach gives convincing results and allows to converge toward a good image segmentation in spite of speckle noise. The rocks and manufactured object shadows are well segmented and close to the result we expected. The cast shadow of a manufactured object (reported in Figure 6.b) has a

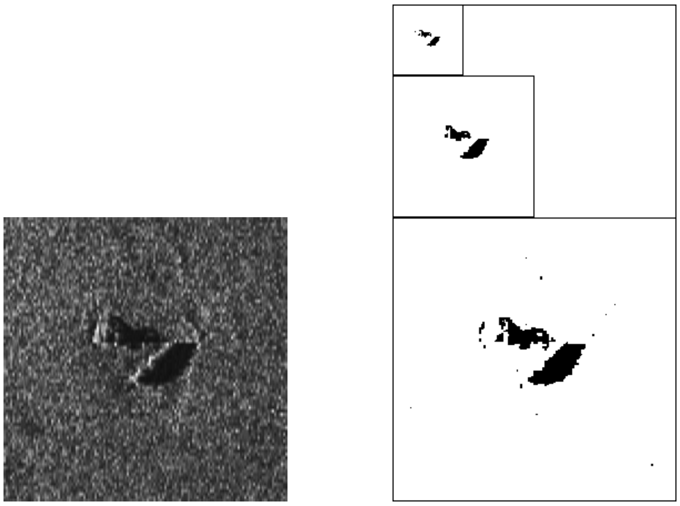

Fig a: *sonar picture (object and rock shadows)* **Fig b**: *Multigrid* **MAP** *segmentation results with parameters obtained with the* **ICE** *procedure*

Fig. 6.

geometric shape easily identifiable for the classification step. This method allows to detect the little rocks (see Figure 7.*e*) and to preserve their shadow shapes at the finest resolution. Nevertheless, we can see in Figure 8.*e* that the proposed algorithm do not permit to eliminate totally the speckle noise effect which induces false small shadow areas. In order to still improve the results, we are now working on unsupervised hierarchical approach with inter-level connections.

7 Conclusion

We have described an unsupervised iterative estimation procedure based on the **ICE** algorithm [1] which offers an appropriate estimation of the noise model and Gibbs distribution parameters. The *Estimation Step* takes into account the diversity of the laws in the distribution mixture of a sonar image and can be used in a global estimation-segmentation procedure in order to solve the hard problem of unsupervised sonar image segmentation. This scheme is computationally simple, exhibits rapid convergence properties and well suited to automatic extraction of information from a large variety of sonar images. This method has been validated on a number of real sonar images demonstrating the efficiency and robustness of this scheme. The extension of the method to unsupervised hierarchical segmentation (with inter-level connections) will be the topic of our next research.

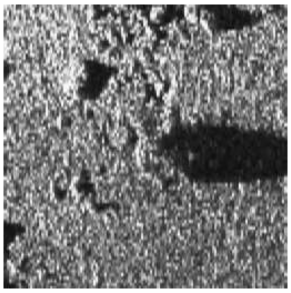

Fig 7.a: *sonar picture (object and rock shadows)*

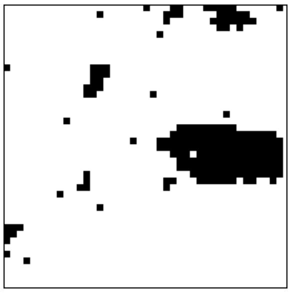

Fig 7.b: *K-means clustering procedure*

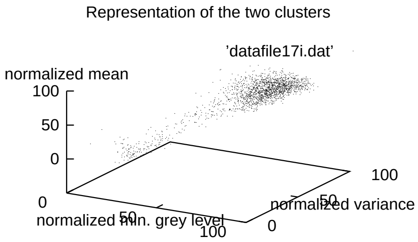

Fig 7.c: *representation of the two clusters*

Initialization : **K-means**				
$\Phi^{[0]}_{y_{(shadow)}}$		$0.11_{(\pi)}$	$34_{(\mu)}$	$149_{(\sigma^2)}$
$\Phi^{[0]}_{y_{(sea-bottom)}}$		$0.89_{(\pi)}$	$39_{(min)}$	$2830_{(\alpha^2)}$
$\Phi^{[0]}_{x}$	$1.2_{(\beta_1)}$	$1.7_{(\beta_2)}$	$-\,0.3_{(\beta_3)}$	$-\,0.2_{(\beta_4)}$

ICE procedure				
$\hat{\Phi}_{y_{(shadow)}}$		$0.10_{(\pi)}$	$28_{(\mu)}$	$34_{(\sigma^2)}$
$\hat{\Phi}_{y_{(sea-bottom)}}$		$0.90_{(\pi)}$	$39_{(min)}$	$4960_{(\alpha^2)}$
$\hat{\Phi}_{x}$	$1.2_{(\beta_1)}$	$1.7_{(\beta_2)}$	$-\,0.2_{(\beta_3)}$	$-\,0.2_{(\beta_4)}$

Table 3: *estimated parameters on the picture reported in Figure 7.a. π stands for the proportion of the two classes within the sonar image. μ and σ^2 are the Gaussian parameters (shadow area). min and α are the Rayleigh law parameters (sea floor reverberation). β_i's are the a priori parameters of the Markovian modeling. $\Phi^{[0]}$ represents the initial parameter estimates and the final estimates are denoted $\hat{\Phi}$.*

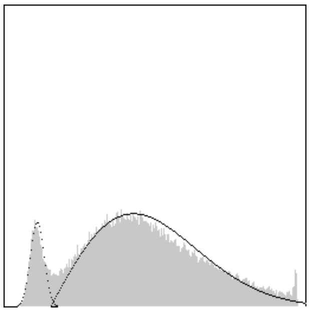

Fig 7.d: *Image histogram of the picture reported in Figure 7.a and estimated mixture*

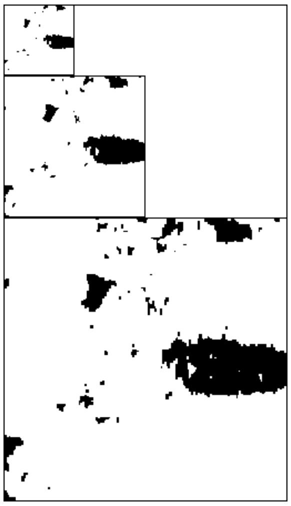

Fig 7.e: *Multigrid* **MAP** *segmentation estimates with parameters obtained with the* **ICE** *procedure*

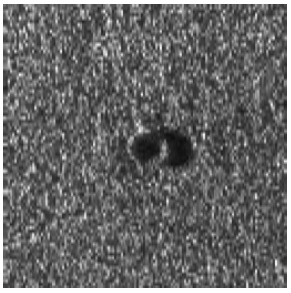

Fig 8.a: *sonar picture (sandy sea floor and a tyre)*

Fig 8.b: *K-means clustering procedure*

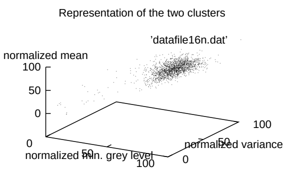

Fig 8.c: *representation of the two clusters*

Initialization : **K-means**				
$\hat{\Phi}^{[0]}_{y_{(shadow)}}$	$0.35_{(\pi)}$	$78_{(\mu)}$	$406_{(\sigma^2)}$	
$\hat{\Phi}^{[0]}_{y_{(sea-bottom)}}$	$0.65_{(\pi)}$	$46_{(min)}$	$1640_{(\alpha^2)}$	
$\hat{\Phi}^{[0]}_{x}$	$1.0_{(\beta_1)}$	$1.5_{(\beta_2)}$	$-0.16_{(\beta_3)}$	$-0.2_{(\beta_4)}$

ICE procedure				
$\hat{\Phi}_{y_{(shadow)}}$	$0.03_{(\pi)}$	$36_{(\mu)}$	$84_{(\sigma^2)}$	
$\hat{\Phi}_{y_{(sea-bottom)}}$	$0.97_{(\pi)}$	$46_{(min)}$	$1879_{(\alpha^2)}$	
$\hat{\Phi}_{x}$	$1.5_{(\beta_1)}$	$1.7_{(\beta_2)}$	$-0.3_{(\beta_3)}$	$-0.6_{(\beta_4)}$

Table 4: *estimated parameters on the picture reported in Figure 8.a. π stands for the proportion of the two classes within the sonar image. μ and σ^2 are the Gaussian parameters (shadow area). min and α are the Rayleigh law parameters (sea floor reverberation). β_i's are the a priori parameters of the Markovian modeling. $\Phi^{[0]}$ represents the initial parameter estimates and the final estimates are denoted $\hat{\Phi}$.*

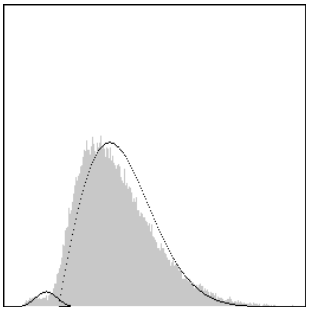

Fig 8.d: *Image histogram of the picture reported in Figure 8.a and estimated mixture*

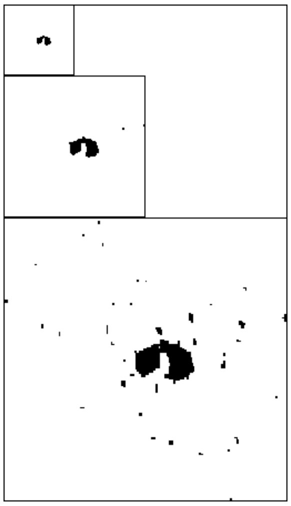

Fig 8.e: *Multigrid* **MAP** *segmentation results with parameters obtained with the* **ICE** *procedure*

References

1. F. Salzenstein and W.Pieczinsky. Unsupervised bayesian segmentation using hidden markovian fields. *In proc. ICASSP'95*, pages 2411–2414, May 1995.
2. H. Derin and H. Elliot. Modeling and segmentation of noisy and textured images using Gibbs random fields. *IEEE Trans. Pattern Anal. and Machine Intell.*, PAMI-9(1):39–55, January 1987.
3. F. Schmitt, M. Mignotte, C. Collet, and P. Thourel. Estimation of noise parameters on sonar images. In *Signal and Image Processing, SPIE'96*, volume 2823, pages 1–12, Denver, Colorado, USA, August 1996.
4. J. Besag. On the statistical analysis of dirty pictures. *Journal of the Royal Statistical Society*, B-48:259–302, 1986.
5. C. Collet, P. Thourel, P. Pérez, and P. Bouthemy. Hierarchical MRF modeling for sonar picture segmentation. In *proc. ICIP'96*, Lausanne, September 1996.
6. S. Lakshmanan and H. Derin. Simultaneous parameter estimation and segmentation of Gibbs random fields using simulated annealing. *IEEE Trans. on PAMI*, 11(8):799–813, August 1989.
7. J.G. Postaire and P.A. Vasseur. An approximate solution to normal mixture identification with application to unsupervised pattern classification. *IEEE Trans. on PAMI*, (2):163–179, 1981.
8. G. Celleux and J. Diebolt. A random imputation principle : the stochastic EM algorithm. Technical Report 901, INRIA, September 1988.
9. A.P. Dempster, N.M. Laird, and D.B. Rubin. Maximum likelihood from incomplete data via the EM algorithm. *Royal Statistical Society*, pages 1–38, 1976.
10. Z. Kato, J. Zerubia, and M. Berthod. Unsupervised parallel image classification using a hierarchical Markovian model. In *Proc. ICCV'95*, volume 1, pages 169–174, Cambridge, Massachusetts, 20-23 June 1995.
11. B. Chalmond. An iterative gibbsian technique for reconstruction of m-ary images. *Pattern Recognition*, 22(6):747–761, 1989.
12. M. Mignotte. Modèle markovien: estimation des paramètres. Technical Report 7, Ecole Navale, March 1996.
13. Y. Kim and H.S Yang. Efficient image labelling based on Markov random field and error backpropagation network. *Pattern Recognition*, 26(11):1695–1707, 1993.
14. P. A. Kelly, H. Derin, and K. D. Hart. Adaptative segmentation of speckled images using a hierarchical random field model. *IEEE Transactions on Acoustic Speech and Signal Processing*, 36(10):1628–1641, October 1988.
15. S. Geman and D. Geman. Stochastic relaxation, Gibbs distributions and the Bayesian restoration of images. *IEEE Trans. Pattern Anal. and Machine Intell.*, PAMI-6(6):721–741, November 1984.
16. J. W. Goodman. Some fundamental properties of speckle. *Journal of Optical Society of America*, 66(11):1145–1150, November 1976.
17. L. Younes. Parametric inference for imperfectly observed Gibbsian fields. *Springer-Verlag Prob. Th. Rel. Fields 82*, pages 625–645, 1989.
18. S. Banks. Signal processing image processing and pattern recognition, 1990.
19. B. Braathen, P. Masson, and W. Pieczynski. Global and local methods of unsupervised Bayesian segmentation of images. *GRAPHICS and VISION*, (1):39–52, 1993.
20. F. Heitz, P. Pérez, and P. Bouthemy. Multiscale minimisation of global energy functions in some visual recovery problems. In *Computer Vision Graph. and Image Proces. : Image Understanding*, volume 59, january 1994.